Monthly Notices
of the
ROYAL ASTRONOMICAL SOCIETY

Mon. Not. R. Astron. Soc. **408,** 2115–2127 (2010) doi:10.1111/j.1365-2966.2010.17291.x

A fundamental relation between mass, star formation rate and metallicity in local and high-redshift galaxies

F. Mannucci,[1⋆] G. Cresci,[1,2] R. Maiolino,[3] A. Marconi[4] and A. Gnerucci[4]

[1]*INAF – Osservatorio Astrofisico di Arcetri, Largo E. Fermi 5, I-50125 Firenze, Italy*
[2]*Max-Planck-Institut für extraterrestrische Physik (MPE), Giessenbachstr. 1, D-85748 Garching, Germany*
[3]*INAF – Osservatorio Astronomico di Roma, via di Frascati 33, I-00040 Monte Porzio Catone, Italy*
[4]*Dip. di Fisica e Astronomia, Università di Firenze, Largo E. Fermi 2, I-50125 Firenze, Italy*

Accepted 2010 July 2. Received 2010 July 2; in original form 2010 March 26

ABSTRACT

We show that the mass–metallicity relation observed in the local universe is due to a more general relation between stellar mass $M_\star$, gas-phase metallicity and star formation rate (SFR). Local galaxies define a tight surface in this 3D space, the fundamental metallicity relation (FMR), with a small residual dispersion of ∼0.05 dex in metallicity, i.e. ∼12 per cent. At low stellar mass, metallicity decreases sharply with increasing SFR, while at high stellar mass, metallicity does not depend on SFR.

High-redshift galaxies up to $z \sim 2.5$ are found to follow the same FMR defined by local Sloan Digital Sky Survey (SDSS) galaxies, with no indication of evolution. In this respect, the FMR defines the properties of metal enrichment of galaxies in the last 80 per cent of cosmic time. The evolution of the mass–metallicity relation observed up to $z = 2.5$ is due to the fact that galaxies with progressively higher SFRs, and therefore lower metallicities, are selected at increasing redshifts, sampling different parts of the same FMR.

By introducing the new quantity $\mu_\alpha = \log(M_\star) - \alpha \log(\mathrm{SFR})$, with $\alpha = 0.32$, we define a projection of the FMR that minimizes the metallicity scatter of local galaxies. The same quantity also cancels out any redshift evolution up to $z \sim 2.5$, i.e. all galaxies follow the same relation between $\mu_{0.32}$ and metallicity and have the same range of values of $\mu_{0.32}$. At $z > 2.5$, evolution of about 0.6 dex off the FMR is observed, with high-redshift galaxies showing lower metallicities.

The existence of the FMR can be explained by the interplay of infall of pristine gas and outflow of enriched material. The former effect is responsible for the dependence of metallicity with SFR and is the dominant effect at high redshift, while the latter introduces the dependence on stellar mass and dominates at low redshift. The combination of these two effects, together with the Schmidt–Kennicutt law, explains the shape of the FMR and the role of $\mu_{0.32}$. The small-metallicity scatter around the FMR supports the smooth infall scenario of gas accretion in the local universe.

Key words: galaxies: abundances – galaxies: formation – galaxies: high-redshift – galaxies: starburst.

1 INTRODUCTION

Gas metallicity is regulated by a complex interplay between star formation, infall of metal-poor gas and outflow of enriched material. A relation between magnitude and metallicity was discovered in the 1970s (McClure & van den Bergh 1968; Lequeux et al. 1979), in which more luminous galaxies also have higher metallicities. Later on, it was understood that this luminosity–metallicity relation is a manifestation of a more fundamental stellar mass–metallicity relation where galaxies with larger stellar mass $M_\star$ have higher metallicities (Garnett 2002; Pérez-González et al. 2003; Pilyugin, Vílchez & Contini 2004; Tremonti et al. 2004; Savaglio et al. 2005; Lee et al. 2006; Cowie & Barger 2008; Kewley & Ellison 2008; Liu et al. 2008; Michel-Dansac et al. 2008; Panter et al. 2008; Rodrigues et al. 2008; Hayashi et al. 2009; Pérez-Montero et al. 2009).

The origin of this relation is debated, and many different explanations have been proposed, including ejection of metal-enriched gas (e.g. Edmunds 1990; Lehnert & Heckman 1996; Garnett 2002; Tremonti et al. 2004; Kobayashi, Springel & White 2007; Scannapieco et al. 2008; Spitoni et al. 2010), 'downsizing', i.e. a systematic dependence of the efficiency of star formation with

⋆E-mail: filippo@arcetri.astro.it

galaxy mass (e.g. Brooks et al. 2007; Mouchine et al. 2008; Calura et al. 2009), variation of the initial mass function (IMF) with galaxy mass (Köppen, Weidner & Kroupa 2007) and infall of metal-poor gas (Finlator & Davé 2008; Davé et al. 2010).

Recently, evidence has been found that at high redshift the infall of pristine gas can have a dominant role (Agertz, Teyssier & Moore 2009; Bournaud & Elmegreen 2009; Brooks et al. 2009; Dekel, Sari & Ceverino 2009). The mass–metallicity relation has been studied by Erb et al. (2006) at $z \sim 2.2$ and by Maiolino et al. (2008) and Mannucci et al. (2009) at $z = 3$–4, finding a strong and monotonic evolution, with metallicity decreasing with redshift at a given mass. The same authors (Erb et al. 2006; Erb 2008; Mannucci et al. 2009) have also studied the relation between metallicity and gas fraction, i.e. the effective yields, obtaining clear evidence of the presence of infall in high-redshift galaxies.

Even more recently, Cresci (2010) have obtained the evidence of 'positive' metallicity gradients in a small sample of three disc galaxies at $z = 3.5$, with lower metallicities in more active regions of star formation. The presence of these gradients in galaxies with very regular dynamics can be understood as a consequence of accretion of metal-poor gas, producing a new episode of star formation in older, more metal-rich galaxies.

If infall is at the origin of the star formation activity, and outflows are produced by exploding supernovae (SNe), a relation between metallicity and star formation rate (SFR) is likely to exist. In other words, SFR is a parameter that should be considered in the scaling relations that include metallicity. The role of specific SFR (SSFR) in this content was already studied by Ellison et al. (2008), who presented a mild ($\leq$0.1 dex) dependence of metallicity on SSFR when binning galaxies according to their $M_\star$. Recently, Lopez-Sanchez (2010) also presented evidence of a link between SFR and metallicity, while Peeples, Pogge & Stanek (2009) reported high values of SFR in a sample of outliers, towards low metallicities, of the mass–metallicity relation.

To test the hypothesis of a correlation between SFR and metallicity in the present Universe and at high redshift, we have studied several samples of galaxies at different redshifts whose metallicity, $M_\star$, and SFR have been measured. In the next section we present the data samples we are using for this study. In Section 3 we study the mass–metallicity relation as a function of SFR, and in the following section we introduce the fundamental metallicity relation (FMR). In Section 7 we discuss the physical origin of this relation. We adopt a Λ cold dark matter (ΛCDM) cosmology with $H_0 = 70\ \mathrm{km\,s^{-1}}$, $\Omega_\mathrm{m} = 0.3$ and $\Omega_\Lambda = 0.7$. Stellar mass $M_\star$ and SFR are expressed in $\mathrm{M}_\odot$ and $\mathrm{M}_\odot\ \mathrm{yr}^{-1}$, respectively.

2 THE GALAXY SAMPLES

2.1 $z = 0$: SDSS

Local galaxies are well measured by the Sloan Digital Sky Survey (SDSS) project (Abazajian et al. 2009). We used the MPA/JHU catalogue of emission-line fluxes and stellar masses from SDSS-DR7 available at http://www.mpa-garching.mpg.de/SDSS and described in Kauffmann et al. (2003b), Brinchmann et al. (2004) and Salim et al. (2007). The catalogue includes 927 552 galaxies whose spectroscopic properties, such as emission-line fluxes and spectroscopic indexes, have been measured.

We selected emission-line galaxies with redshift between 0.07 and 0.30 (47 per cent of the total sample). The minimum redshift is set in order to ensure that [O II]λ3727 is well within the useful spectral range, and that the 3-arcsec aperture of the spectroscopic fibre samples a significant fraction of the galaxies (3 arcsec corresponds to $\sim$4 kpc at $z = 0.07$).

A threshold to the signal-to-noise ratio (S/N) of Hα of S/N $>$ 25 was used to have reliable values of metallicity, while no S/N threshold is used for the other lines. Such a high S/N on Hα is needed to ensure that all the main optical lines are generally detected with enough S/N without introducing metallicity biases. For example, the [N II]λ6584 flux is about half of the Hα flux at high metallicities, and about one-tenth at the lowest metallicities sampled by SDSS. Noise and intrinsic dispersion of the [N II]λ6584/Hα ratio could produce very low fluxes of the [N II]λ6584 in low-metallicity galaxies. If a threshold in the S/N of [N II]λ6584 is used, some low-metallicity galaxies would be removed from the sample, while this effect would be negligible among high-metallicity galaxies. As a result a metallicity bias would be introduced, and such a bias can be important when high S/N thresholds are used. Also, this selection bias would be correlated with SFR as more active galaxies have brighter lines. The use of a S/N threshold of 25 on Hα means that, on average, the faintest [N II]λ6584 lines are detected with S/N $>$ 2.5, but even galaxies with lower S/N for this line are included in the sample. This limit on S/N selects 43 per cent of the remaining sample.

We limited dust extinction to $A_V < 2.5$, in order not to deal with very large extinction corrections, and galaxies with Balmer decrements below 2.5 were removed. These selections remove 0.2 per cent of the galaxies. Finally, active galactic nucleus (AGN) like galaxies (22 per cent of the sample) were excluded by using the classification by Kauffmann et al. (2003a).

Total stellar masses $M_\star$ from Kauffmann et al. (2003b) were used, as listed in the same MPA/JHU catalogue, with a correction factor of 1.06 to scale the masses down from a Kroupa (2001) to a Chabrier (2003) IMF.

SFRs inside the spectroscopic aperture were measured from the Hα emission-line flux corrected for dust extinction as estimated from the Balmer decrement. The conversion factor between Hα luminosity and SFR in Kennicutt (1998) was used, corrected to a Chabrier (2003) IMF.

Oxygen gas-phase abundances were measured from the emission-line ratios as described in Nagao, Maiolino & Marconi (2006) and Maiolino et al. (2008). Two independent measurements of metallicity are available for these galaxies, based either on the [N II]λ6584/Hα ratio or on the R23 quantity, defined as R23 = ([O II]λ3727 + [O III]λ4958,5007)/Hβ. When both quantities are inside the useful range for metallicity calibration, i.e. log([N II]λ6584/Hα) < -0.35 and log(R23) < 0.90, we selected only galaxies where the two values of metallicity differ less that 0.25 dex (97 per cent of the sample), and galaxy metallicity is then defined as the average of these two values. The spread of the difference between these two estimates of metallicity is 0.09 dex ($\sim$23 per cent), with a significant albeit small systematic difference of 0.05 dex ($\sim$12 per cent) with the value from R23 systematically higher than that derived from [N II]λ6584/Hα. This small difference is likely to be due to the different sample used here and in Maiolino et al. (2008), which use a S/N threshold of 10 on the flux of each line. This may introduce a small bias in the calibrations relative to our sample.

The final galaxy sample contains 141 825 galaxies.

2.2 $z = 0.5$–2.5

Many galaxies have been observed at high redshift and these data can be used to study the evolution of metallicity with respect to

the other properties of galaxies. We extracted from the literature three samples of galaxies at intermediate redshifts, for a total of 182 objects, having published values of emission-line fluxes, $M_\star$, and dust extinction: $0.5 < z < 0.9$ (Savaglio et al. 2005, GDDS galaxies), $1.0 < z < 1.6$ (Shapley et al. 2005; Liu et al. 2008; Epinat et al. 2009; Wright et al. 2009) and $2.0 < z < 2.5$ (Förster Schreiber et al. 2009; Law et al. 2009; Lehnert et al. 2009). The same procedure used for the SDSS galaxies was applied to these galaxies. Metallicity is estimated either from R23 or from [N II]λ6584/Hα, depending on which lines are available. AGNs are removed using the BPT diagram (Kauffmann et al. 2003a) or, when [O III]λ5007 and Hβ are not available, by imposing $\log([\mathrm{N\,II}]\lambda6584/\mathrm{H}\alpha) < -0.3$. The [N II]λ6584 line, which is usually much fainter than Hα, is not detected in several galaxies, but removing these galaxies from the sample would bias it towards high metallicities. For these objects we have assumed a value of the intrinsic [N II]λ6584 flux which is half of the upper limiting flux. When necessary, the published $M_\star$ have been converted to a Chabrier (2003) IMF. For galaxies without observations of both Hα and Hβ, dust extinction is estimated from spectral energy distribution (SED) fitting, and we assume that continuum and the emission lines suffer the same extinction. In local starburst, lines often suffer of higher extinctions [A_V(lines) $\sim 2.3 A_V$(SED) according to Calzetti et al. (2000)]. We have checked that the inclusion of this effect would have little effect on the final relations and on the conclusions of this paper.

Erb et al. (2006) have observed a large sample of 91 galaxies at $z \sim 2.2$. Metallicities have been measured only on average spectra stacked according to $M_\star$, which has the results of mixing galaxies of different SFRs. Despite this problem, no systematic differences in metallicity are detected with respect to the other galaxies measured individually, and the Erb et al. (2006) galaxies are included in the high-redshift sample, although without binning them with the rest of the galaxies.

2.3 $z = 3$–4

A significant sample of 16 galaxies at redshift between 3 and 4 was observed by Maiolino et al. (2008) and Mannucci et al. (2009) for the LSD and AMAZE projects. Published values of stellar masses, line fluxes and metallicities are available for these galaxies, which can be compared with lower redshift data. The same procedure as at lower redshift was used, with the exception that SFR is estimated from Hβ after correction for dust extinction, and metallicities are measured by a simultaneous fitting of the line ratios involving [O II]λ3727, Hβ and [O III]λ4958, 5007, as described in Maiolino et al. (2008).

3 THE MASS–METALLICITY RELATION AS A FUNCTION OF SFR

The grey-shaded area in the left-hand panel of Fig. 1 shows the mass–metallicity relation for our sample of SDSS galaxies. Despite the differences in the selection of the sample and in the measure of metallicity, our results are very similar to what has been found by Tremonti et al. (2004). The metallicity dispersion of our sample, ∼0.08 dex, is somewhat smaller to what have been found by these authors, ∼0.10 dex, possibly due to different sample selections and metallicity calibration. The fourth-order polynomial fit to the median mass–metallicity relation is

$$12 + \log(\mathrm{O/H}) = 8.96 + 0.31m - 0.23m^2 - 0.017m^3 + 0.046m^4, \quad (1)$$

where $m = \log(M_\star) - 10$ in solar units.

We have computed the median metallicity of SDSS galaxies for different values of SFR. Median has been computed in bins of mass and SFR of 0.15 dex width in both quantities. On average, each bin contains 760 galaxies, and only bins containing more than 50 galaxies are considered. The left-hand panel of Fig. 1 also shows these median metallicities as a function of $M_\star$. It is evident that a systematic segregation in SFR is present in the data. While galaxies with high $M_\star$ [$\log(M_\star) > 10.9$] show no correlation between metallicity and SFR, at low $M_\star$ more active galaxies also show lower metallicity. The same systematic dependence of metallicity on SFR can be seen in the right-hand panel of Fig. 1, where metallicity is plotted as a function of SFR for different values of mass. Galaxies with high

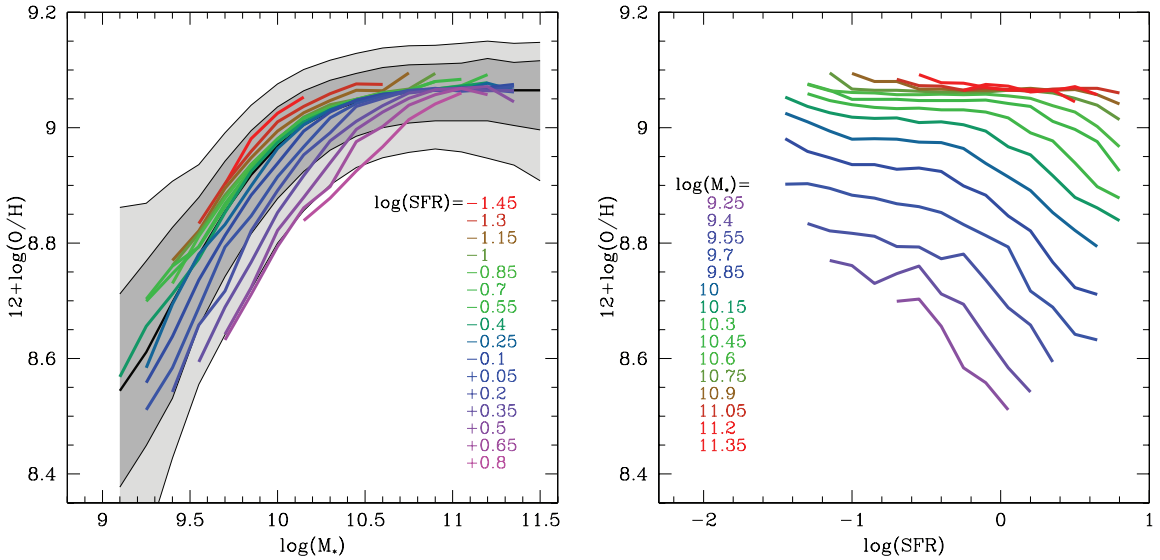

Figure 1. Left-hand panel: the mass–metallicity relation of local SDSS galaxies. The grey-shaded areas contain 64 and 90 per cent of all SDSS galaxies, with the thick central line showing the median relation. The coloured lines show the median metallicities, as a function of $M_\star$, of SDSS galaxies with different values of SFR. Right-hand panel: median metallicity as a function of SFR for galaxies of different $M_\star$. At all $M_\star$ with $\log(M_\star) < 10.7$, metallicity decreases with increasing SFR at constant mass.

SFRs show a sharp dependence of metallicity on SFR, while less active galaxies show a less pronounced dependence.

A hint of this effect was already noted by Ellison et al. (2008), but the different sample selection and the large bins in SFR reduced the observed dependence on SFR to a small correction of ∼0.05 dex with respect to the value determined by the mass–metallicity relation. Also Rupke, Veilleux & Baker (2008) presented evidences for lower metallicities in local galaxies with high SFRs, although with a very large scatter.

4 THE FUNDAMENTAL METALLICITY RELATION

The dependence of metallicity on $M_\star$ and SFR can be better visualized in a 3D space with these three coordinates, as shown in Fig. 2. SDSS galaxies appear to define a tight surface in the space, the FMR, with metallicity well defined by the values of $M_\star$ and SFR. All the data on this FMR are shown in Table 1.

The introduction of the FMR results in a significant reduction of residual metallicity scatter with respect to the simple mass–metallicity relation. The dispersion of individual SDSS galaxies around the FMR, shown in Fig. 3, computed in bins of 0.05 dex in $M_\star$ and SFR, is ∼0.06 dex when computed across the full FMR and reduces to ∼0.05 dex, i.e. about 12 per cent, in the central part of the relation where most of the galaxies are found. This means that about half of the total scatter of the mass–metallicity relation (0.08 dex) is due to the systematic effect with SFR, while about half is due to intrinsic differences between galaxies and/or uncertainties on the measurements. The reduction in scatter becomes even more significant when considering that most of the galaxies in the sample cover a small range in SFR, with 64 per cent of the galaxies ($\pm 1\sigma$) contained inside 0.8 dex. Galaxies with very low SFRs are not selected due to the high S/N threshold on Hα, while high-SFR galaxies are rare in the local universe. As a consequence the scatter on the full sample is dominated by galaxies having a small correction due to SFR. In contrast, considering only galaxies with high SFRs, the scatter is reduced by a large factor. For example, for log(SFR) > 0.5, the scatter around the average mass–metallicity relation is about 40 per cent, while it is a factor of ∼3 lower around the FMR.

The final scatter is consistent with the intrinsic uncertainties in the measure of metallicity (∼0.03 dex for the calibration, to be added to the uncertainties in the line ratios), on mass (estimated to be 0.09 dex by Tremonti et al. 2004) and on the SFR, which are dominated by the uncertainties on dust extinction. Nevertheless, the scatter around FMR tends to reduce when the minimum redshift $z_{\rm min}$ of the galaxy sample is increased. This means that part of the residual scatter is probably due to the different apertures used to measure mass, based on a total magnitude, and metallicity and SFR, derived for the central 3 arcsec. In particular, the effect of metallicity gradients are expected to become less important at larger redshifts, and for this reason the increase of $z_{\rm min}$ is able to reduce the scatter.

A close inspection of Fig. 3 reveals the presence of an extended wing towards lower metallicities in the distribution of scatter. This extension contains ∼3 per cent of the objects. Most of these galaxies have low $M_\star$ and high SSFR, and could be objects in special conditions. For example, they could be interacting galaxies, which will be discussed in Section 7.

We have fitted the median values of metallicity of the SDSS galaxies in Table 1 with a second-order polynomial in $M_\star$ and SFR, obtaining

$$12 + \log({\rm O/H}) = 8.90 + 0.37m - 0.14s - 0.19m^2 + 0.12ms - 0.054s^2, \quad (2)$$

where $m = \log(M_\star) - 10$ and $s = \log({\rm SFR})$ in solar units. The residual scatter of median metallicities around this fit is 0.001 dex. Such a fit, shown in Fig. 2, provides a clear representation of the dependence of metallicity both on $M_\star$ and SFR, and allows us to compare the local FMR with high-redshift galaxies.

The shape of the FMR surface depends on a number of factors, such as the selection of the galaxy sample and the way metallicity, $M_\star$ and SFR are measured. We have done a number of checks to test whether the result depends critically on either of our assumptions. First, we changed the thresholds in S/N and redshift used to select the galaxy sample, and checked that the results do not change systematically with these thresholds. Secondly, we have studied the effect of considering only metallicities derived either from R23 or from [N II]λ6584/Hα. As discussed in Section 2.1, systematic differences are found but are limited to the level of 0.05 dex. Apart from this metallicity offset, the shape of the FMR does not change by more than 0.05 dex at any point. In particular, there is no large, monotonic dependence of the difference with SFR or SSFR. This is interesting because there could be systematic effects related either to the density of the H II regions or to the ionization parameter U, which could depend on the SSFR (e.g. Shapley et al. 2005; Hainline et al. 2009) and introduce spurious behaviour. R23 and [N II]λ6584/Hα show opposite dependencies with U (see e.g. Liu et al. 2008 and Nagao et al. 2006). For this reason the absence of systematic differences between these two line ratios with SSFR is an indication that the dependence of measured metallicity on density or U, if present, is small, in agreement with the findings of Liu et al. (2008) and Brinchmann, Pettini & Charlot (2008).

There are two points that could affect the shape of the FMR. First, SFR is estimated from Hα luminosity corrected for extinction using the Balmer decrement. Several authors (Kennicutt 1998; Moustakas, Kennicutt & Tremonti 2006) have shown that this is a reliable SFR indicator over a large range of galaxy properties. Others (Charlot & Longhetti 2001; Brinchmann et al. 2004) have discussed that systematic effects with mass and metallicity could be present. As we have split galaxies in bins of mass and SFR, and inside each bin metallicity spans a small range, any systematic effect on SFR does not hamper the existence of the FMR but could change its shape. Secondly, we are using SFRs and metallicities that apply only to the central 3 arcsec of the galaxies, corresponding to 4–11 kpc projected angular size given our redshift range. These quantities are compared with total mass derived from integrated photometry[1] (Kauffmann et al. 2003b; Salim et al. 2007). In the SDSS sample, the fraction of mass contained inside the projected fibre aperture (as listed in the MPE/JHU catalogue) is about one-third of the total, with log(total mass) – log(fibre mass) = 0.50 ± 0.15, and no systematic dependence on mass. We find that total and fibre mass are correlated with SFR and metallicity at a similar degree, and we used the total mass as this is the quantity usually available in galaxy catalogues. The measured metallicity is expected to be a fair representation of total metallicity: abundance gradients can be present but, at least in local galaxies, they are of modest importance in this context, both because only weak variations with radius are usually found (e.g. Magrini et al. 2009) and because our apertures sample a significant part of the galaxies. Correcting fibre

[1] See http://www.mpa-garching.mpg.de/SDSS/DR7/masscomp.html

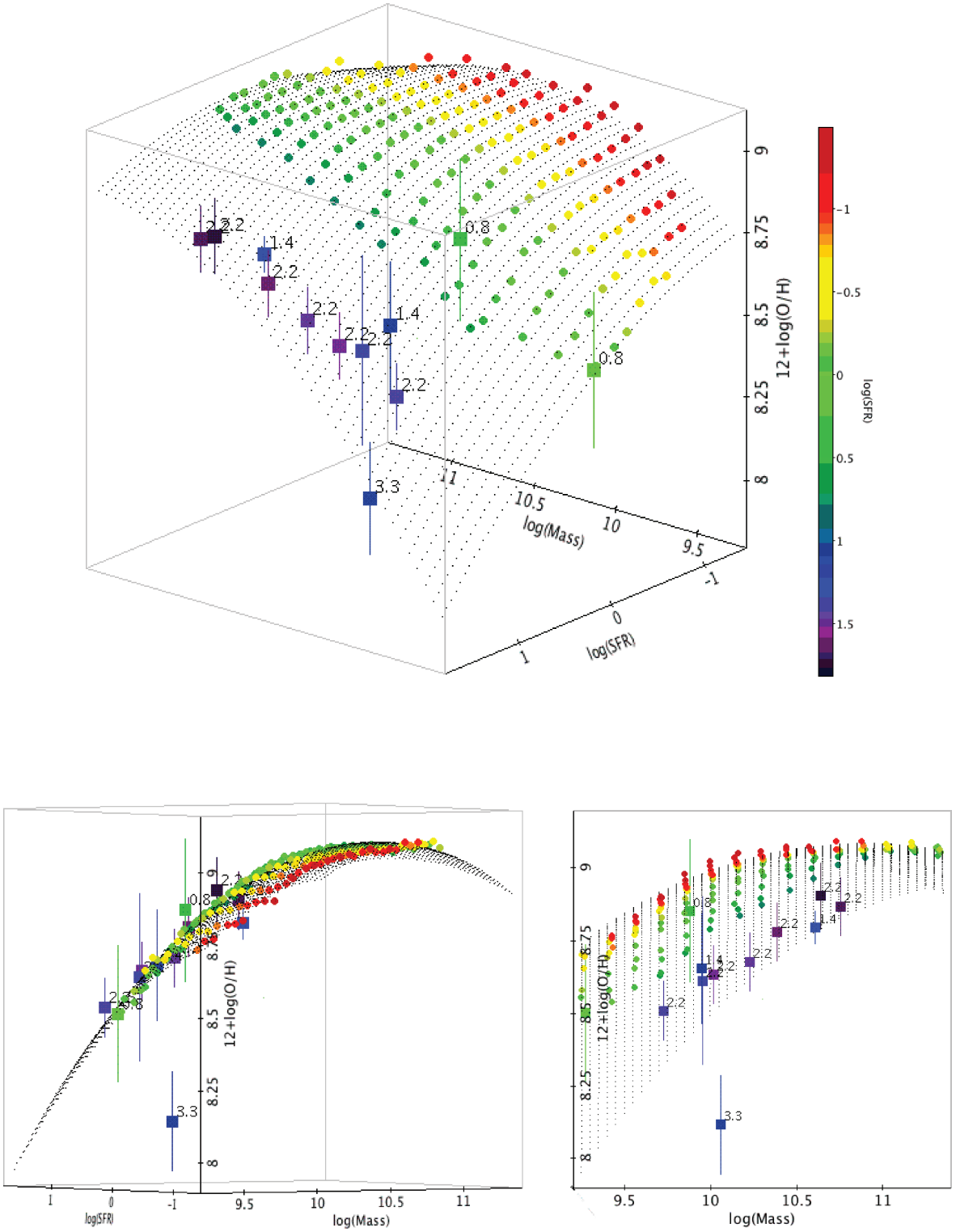

Figure 2. Three projections of the FMR among $M_\star$, SFR and gas-phase metallicity. Circles without error bars are the median values of metallicity of local SDSS galaxies in bin of $M_\star$ and SFR, colour-coded with SFR as shown in the colour bar on the right-hand side. These galaxies define a tight surface in the 3D space, with dispersion of single galaxies around this surface of ∼0.05 dex. The black dots show a second-order fit to these SDSS data, extrapolated towards higher SFR. Square dots with error bars are the median values of high-redshift galaxies, as explained in the text. Labels show the corresponding redshifts. The projection in the lower left-hand panel emphasizes that most of the high-redshift data, except the point at $z = 3.3$, are found on the same surface defined by low-redshift data. The projection in the lower right-hand panel corresponds to the mass–metallicity relation, as in Fig. 1, showing that the origin of the observed evolution in metallicity up to $z = 2.5$ is due to the progressively increasing SFR.

Table 1. The FMR for SDSS galaxies selected as in Section 2.1. For each value of $M_\star$ (reported in the first line) and SFR (first column) we list the median value of metallicity, the 1σ dispersion around this value, and the number of galaxies in each bin.

log(SFR)	log($M_\star$)															
	9.10	9.25	9.40	9.55	9.70	9.85	10.00	10.15	10.30	10.45	10.60	10.75	10.90	11.05	11.20	11.35
−1.45					8.90	8.98	9.02	9.05								
					0.08	0.07	0.06	0.07								
					88	116	94	68								
−1.30				8.83	8.90	8.96	9.01	9.04	9.06	9.08	9.09					
				0.07	0.07	0.07	0.06	0.06	0.06	0.07	0.08					
				99	227	385	460	339	224	95	54					
−1.15			8.77	8.82	8.90	8.95	8.99	9.03	9.05	9.07	9.07	9.09				
			0.07	0.08	0.07	0.07	0.07	0.06	0.06	0.07	0.08	0.07				
			58	159	389	694	881	818	672	414	214	73				
−1.00			8.76	8.82	8.88	8.94	8.98	9.02	9.04	9.05	9.06	9.07	9.09			
			0.11	0.07	0.07	0.07	0.06	0.06	0.06	0.06	0.07	0.07	0.07			
			76	233	602	958	1226	1455	1331	922	470	224	80			
−0.85			8.73	8.81	8.88	8.94	8.98	9.02	9.04	9.05	9.06	9.06	9.08			
			0.11	0.08	0.08	0.07	0.06	0.06	0.06	0.06	0.06	0.06	0.07			
			120	316	662	1152	1639	1898	1996	1514	966	467	162			
−0.70		8.70	8.75	8.79	8.87	8.93	8.98	9.02	9.03	9.05	9.06	9.07	9.08	9.09		
		0.13	0.10	0.08	0.08	0.08	0.06	0.06	0.06	0.06	0.06	0.06	0.06	0.06		
		71	165	341	705	1223	1809	2214	2550	2338	1650	913	334	128		
−0.55		8.70	8.76	8.79	8.86	8.93	8.98	9.01	9.03	9.05	9.06	9.06	9.07	9.07	9.09	
		0.10	0.11	0.10	0.08	0.07	0.07	0.06	0.05	0.05	0.05	0.06	0.06	0.06	0.06	
		82	195	368	654	1130	1703	2296	2743	2955	2503	1671	815	271	84	
−0.40	8.56	8.65	8.71	8.77	8.85	8.92	8.97	9.01	9.03	9.05	9.06	9.06	9.07	9.07	9.08	
	0.12	0.10	0.11	0.10	0.09	0.08	0.07	0.06	0.06	0.05	0.05	0.05	0.05	0.06	0.06	
	63	123	182	367	628	1010	1509	2100	2826	3186	3005	2197	1257	497	148	
−0.25		8.58	8.69	8.78	8.83	8.90	8.96	9.01	9.03	9.05	9.06	9.06	9.07	9.07	9.08	9.06
		0.12	0.12	0.10	0.10	0.09	0.08	0.07	0.05	0.05	0.05	0.05	0.05	0.05	0.06	0.05
		108	177	324	550	734	1113	1673	2327	2826	2830	2466	1598	721	236	57
−0.10		8.56	8.64	8.74	8.81	8.88	8.94	8.99	9.03	9.05	9.06	9.06	9.07	9.07	9.07	9.07
		0.09	0.13	0.11	0.09	0.09	0.08	0.07	0.06	0.05	0.05	0.05	0.05	0.05	0.06	0.05
		76	115	284	405	580	837	1335	1693	2204	2464	2246	1594	803	293	61
+0.05		8.51	8.58	8.69	8.79	8.85	8.92	8.97	9.02	9.04	9.06	9.07	9.07	9.07	9.07	9.07
		0.12	0.13	0.10	0.11	0.09	0.08	0.07	0.06	0.05	0.05	0.05	0.05	0.05	0.06	0.06
		49	98	151	287	416	591	816	1178	1446	1831	1760	1388	810	332	103
+0.20			8.53	8.66	8.72	8.82	8.89	8.96	8.99	9.04	9.05	9.07	9.07	9.06	9.07	9.06
			0.12	0.12	0.10	0.09	0.09	0.08	0.07	0.05	0.05	0.05	0.04	0.05	0.05	0.06
			63	110	179	327	384	530	740	913	1104	1179	944	622	307	103
+0.35				8.59	8.69	8.77	8.85	8.92	8.98	9.01	9.04	9.06	9.07	9.07	9.07	9.06
				0.11	0.10	0.10	0.08	0.07	0.07	0.06	0.05	0.04	0.04	0.05	0.05	0.05
				65	116	224	296	360	385	559	703	708	658	428	200	66
+0.50					8.64	8.72	8.82	8.88	8.94	9.00	9.03	9.05	9.07	9.07	9.08	
					0.12	0.11	0.09	0.08	0.07	0.06	0.05	0.05	0.04	0.04	0.04	
					92	137	202	236	267	308	368	384	356	232	98	
+0.65					8.63	8.71	8.79	8.86	8.90	8.97	9.00	9.04	9.06	9.07	9.05	
					0.12	0.12	0.08	0.07	0.08	0.07	0.06	0.05	0.04	0.04	0.04	
					55	77	98	146	136	158	162	187	154	131	62	
+0.80								8.84		8.93	8.98	9.02	9.04			
								0.10		0.07	0.06	0.06	0.04			
								63		85	68	68	72			

SFR into total ones is not straightforward as there is no guarantee that Hα scales radially as luminosity or mass. If SFR scales with radius as mass, we expected that total SFR are three times larger than the fibre ones considered here. The use of total SFR would produce a FMR shifted towards higher SFRs, and its shape could have some changes. Nevertheless the small scatter observed in the FMR means that the fibre SFR must be well correlated with the total one.

Summarizing, even if the overall shape of the FMR can change in different samples of galaxies and depends on several details, the main properties of the FMR are very robust and passed all our tests.

5 THE LOCAL FMR AND HIGH-REDSHIFT GALAXIES

Using the samples described in Sections 2.2 and 2.3 we compare the dependence of metallicity on $M_\star$ and SFR in galaxies at $z \sim 0.8$, 1.4, 2.2 and 3.3, and compare it with the properties of local SDSS galaxies. Galaxies at all redshifts follow well-defined mass–metallicity relations (see e.g. Mannucci et al. 2009, and references therein). For this reason each of these samples, except the one at $z \sim 3.3$ that contains 16 objects only, is divided into two equally numerous samples of low- and high-$M_\star$ objects. Median

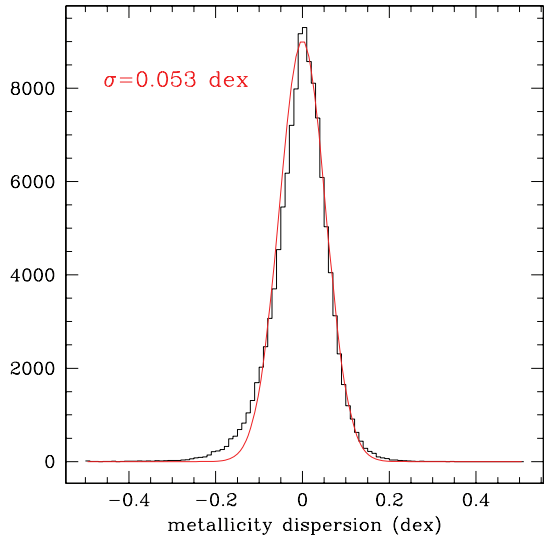

Figure 3. Metallicity dispersion of single SDSS galaxies around the FMR. This histogram shows the differences from the median computed in bins of 0.05 dex in $M_\star$ and SFR. The red line is a Gaussian with $\sigma = 0.053$ dex. Positive differences mean metallicities of single galaxies larger than the median.

values of $M_\star$, SFR and metallicities are computed for each of these samples.

Galaxies at intermediate and high redshifts show, on average, larger SFR with respect to local SDSS galaxies. This is easily explained by selection, because only galaxies with significant SFRs are selected and observed spectroscopically. Galaxies at $z \sim 0.8$ have values of $M_\star$ and SFR which overlap with the SDSS sample, and therefore the two samples can be directly compared. These galaxies are found to be completely consistent with the FMR defined by SDSS galaxies, with no evidence for evolution. This is shown in Figs 2 and 4. At redshift above 1, some extrapolation towards higher SFRs of the fit in equation (2) is required. All galaxies are within 0.6 dex from the most active SDSS galaxies, while most massive galaxies at $z = 2.2$ require an extrapolation of 1 dex. For comparison, SDSS galaxies span two orders of magnitude in SFR (see Fig. 4). The necessity of an extrapolation introduces some uncertainty, but we have checked that the result does not depend critically on the characteristic of the fit, such as the degree of the used polynomial.

When taking into account the uncertainties, data up to $z \sim 2.5$ are consistent, both in shape and in normalization, with the same FMR defined by SDSS, with no evidence for evolution. Distant galaxies show larger dispersions than the local SDSS galaxies, between 0.2 and 0.3 dex. At least part of these relatively larger dispersions are due to the large uncertainties in the estimates of both metallicity and SFR, but part of it could be intrinsic, related to different evolutionary stages of the galaxies. A larger sample of well-measured galaxies is needed to address this point.

The existence of a relation between mass, SFR and metallicity could be considered a mere consequence of the existence of two other well-known relations, the mass–metallicity relation and the mass–SFR relation (see e.g. Schiminovich et al. 2007). In fact, the novelty of this relation can be understood by comparing the relative redshift evolutions: while both the mass–metallicity and the mass–SFR relations are known to evolve significantly with redshift (Daddi et al. 2007; Förster Schreiber et al. 2009; Mannucci et al. 2009), the FMR remains the same up to $z = 2.5$, a period of time spanning 80 per cent of the universe's lifetime. Under this respect, the FMR seems to be the fundamental one, directly related to the mechanisms of galaxy formation. Also, the FMR is not directly related to the mass–SFR relation, as the latter only defines how the FMR is populated.

In the SDSS sample, metallicity changes more with $M_\star$ (∼0.5 dex from one extreme to the other at constant SFR, see Fig. 1) than with SFR (∼0.30 dex at constant mass). Therefore mass is the main

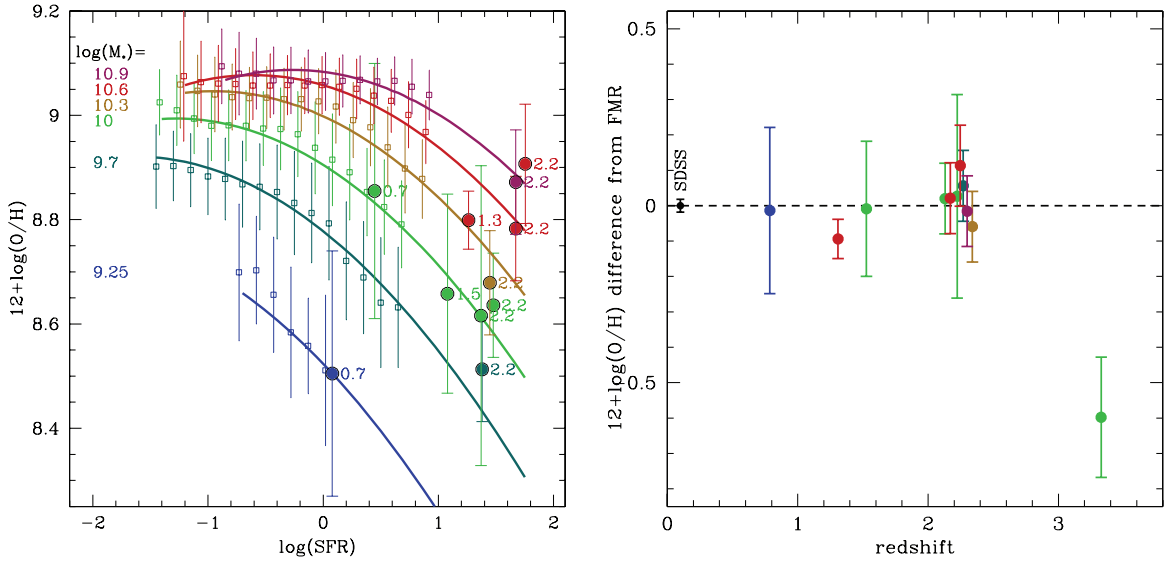

Figure 4. Left-hand panel: metallicity as a function of SFR for galaxies in the bins of $M_\star$ containing high-redshift galaxies. The values of $\log(M_\star)$ are shown by the labels on the left-hand side. Empty square dots are the median values of metallicity of local SDSS galaxies, with error bars showing 1σ dispersions. Lines are the fits to these data. Solid dots are median values for high-redshift galaxies with $z < 2.5$ in the same mass bins, with labels showing redshifts. Right-hand panel: metallicity difference from the FMR for galaxies at different redshifts, colour-coded in mass as in the left-hand panel. The SDSS galaxies defining the relation are showing at $z \sim 0.1$ with their dispersion around the FMR. All the galaxy samples up to $z = 2.5$ are consistent with no evolution of the FMR defined locally. Metallicities lower by ∼0.6 dex are observed at $z \sim 3.3$.

driver of the level of chemical enrichment of SDSS galaxies. This is related to the fact that galaxies with high SFRs, the objects showing the strongest dependence of metallicity on SFR (see the right-hand panel of Fig. 1), are quite rare in the local universe. At high redshifts, mainly active galaxies are selected and the dependence of metallicity on SFR becomes dominant.

5.1 Possible effects on data at $z > 2.5$

Galaxies at $z \sim 3.3$ show metallicities lower by about 0.6 dex with respect to both the FMR defined by the SDSS sample and galaxies at $0.5 < z < 2.5$. This is an indication that some evolution of the FMR appears at $z > 2.5$, although its size can be affected several potential biases of different nature that should be taken into careful account.

First, metallicity at $z = 3.3$ is measured by the oxygen indicators only, while SDSS galaxies use both R23 and [N II]λ6584/Hα. As discussed in Section 2.3, in the local universe both indicators give consistent results, with systematic differences limited to 0.05 dex. Also, galaxies at $z \sim 0.8$ use the same metallicity based on R23. Therefore this is not likely to be the origin of the evolution of 0.6 dex, although it could be responsible for part of the difference.

Secondly, systematic evolution with redshift of the photoionization conditions could be present, for example because high-redshift galaxies have larger SFRs. The presence of such an effect can be studied by comparing different line ratios, and several studies up to $z \sim 2.5$ indicate that such an evolution actually exists (Shapley et al. 2005; Erb et al. 2006; Brinchmann et al. 2008; Liu et al. 2008; Hainline et al. 2009). Nevertheless, this effect is not large enough to move galaxies up to $z = 2.2$ off the FMR, even if some of these galaxies have SFR larger than most of the galaxies at $z = 3.3$. This is in agreement with the results by Liu et al. (2008) and Brinchmann et al. (2008) who estimate a minor effect of this evolution on the measure of metallicity. Therefore evolution of the conditions could give some contribution to the observed evolution but are not likely to be the only reason.

Thirdly, at $z = 3.3$ the Hα and [N II]λ6584 lines fall at ∼2.8 μm and are not observed in any galaxy of this group. For this reason we cannot use this line ratio to remove AGNs. X-ray and mid-infrared data on these targets have been analysed in order to exclude dominant AGN (Maiolino et al. 2008), but it is possible that some faint AGN is still present among these galaxies (Wright et al. 2010). The presence of such objects would tend to reduce the measured metallicity. As almost all galaxies at $z \sim 3$ have metallicity below both the FMR and the mean values at $z \sim 2$ (Mannucci et al. 2009), this effect can explain the observed difference only if AGNs are present in most galaxies.

Fourthly, observations at $z \sim 3.3$ target the [O III]λ5007 line, which has a strong dependence on metallicity, with more metal-poor regions emitting a brighter [O III]λ5007 line for a given SFR (Maiolino et al. 2008). As only the brightest part of the galaxies are detected in our data, this effect could bias the measured line ratios towards the regions of lower metallicities. At lower redshift this effect could be less important, both because [O III]λ5007 is usually intrinsically fainter than Hα observed at $z < 2$, and because the cosmological dimming of the surface brightness, proportional to $(1+z)^4$, is a much more severe problem at higher redshift. In our data at $z = 3.3$, metallicity does not seem to increase with increasing photometric aperture, although we are limited by the low S/N in the external regions of the galaxies. This effect could be present but is not likely to produce the observed difference of a factor of 3.

Finally, there could be selection effects resulting in a reduction of the average metallicity of observed sample. For example, if more metal-rich galaxies also have larger amounts of dust, it is possible that our ultraviolet (UV) selected galaxies at $z \sim 3.3$ preferentially select low-metallicity objects with lower dust column densities. If present, this effect would also work at lower redshift, introducing some evolution also at $z = 2.2$. Again, such an effect could be present but is unlikely to produce a strong differential evolution between $z = 2.2$ and 3.3.

In conclusion, even if the size of the evolution at $z = 3.3$ could be affected by several problems, it is unlikely to be totally due to observational biases.

6 A PROJECTION OF THE FMR THAT REMOVE SECONDARY DEPENDENCIES

At a given mass, galaxies with higher SFR have lower metallicities and therefore have the metallicity properties of lower mass galaxies. As a consequence, we expect that a combination of $M_\star$ and SFR could be better correlated with metallicity. This can be seen in the central panel of Fig. 2, showing a projection of the FMR which considerably reduces the metallicity scatter. To investigate this point we introduce a new quantity μ_α obtained as linear combination of SFR and $M_\star$ as

$$\mu_\alpha = \log(M_*) - \alpha \log(\mathrm{SFR}), \tag{3}$$

where α is a free parameter. For $\alpha = 0$, μ_0 corresponds to $\log(M_\star)$, while for $\alpha = 1$, $\mu_1 = -\log(\mathrm{SSFR})$.

The value of α that minimizes the scatter of median metallicities of SDSS galaxies around the relation corresponds to the quantity μ_α that is more directly correlated with metallicity. Fig. 5 shows the scatter of data in Table 1 as a function of α. These results show that neither $M_\star$ ($\alpha = 0$) nor SSFR ($\alpha = 1$) is the quantity producing the smallest scatter. In fact, $\alpha \sim 0.32$ produces a minimum in the dispersion. The resulting diagram is shown in the right-hand panel of Fig. 5, where metallicity is plotted against $\mu_{0.32}$. The median of the resulting distribution can be fitted by

$$12 + \log(\mathrm{O/H}) = 8.90 + 0.39x - 0.20x^2 - 0.077x^3 + 0.064x^4, \tag{4}$$

where $x = \mu_{0.32} - 10$.

Even if the minimization is computed with SDSS galaxies only, it turns out that high-redshift galaxies up to $z = 2.5$ follow the same relation between $\mu_{0.32}$ and metallicity as in the local universe, and also have the same range of values of $\mu_{0.32}$. This is the same effect noted in the previous section, where high-redshift galaxies have been found to follow the extrapolation of the FMR, but with two important changes: first, no extrapolation from the SDSS galaxies is now needed because both samples have similar values of $\mu_{0.32}$; secondly, it is possible to search for simple physical interpretation of $\mu_{0.32}$ in terms of the physical processes in place.

In practice, metallicity of star-forming galaxies of any mass, any SFR and at any redshift up to $z = 2.5$ follow the following relation:

$$\begin{aligned} 12 + \log(\mathrm{O/H}) &= 8.90 + 0.47x \quad \text{if } \mu_{0.32} < 10.2 \\ &= 9.07 \qquad\quad\ \ \text{if } \mu_{0.32} > 10.5 \end{aligned} \tag{5}$$

with $x = \mu_{0.32} - 10$.

6.1 Metallicity and SSFR

It is interesting to plot metallicity as a function of SSFR, as in Fig. 6, because several properties of galaxies depend on this quantity. In

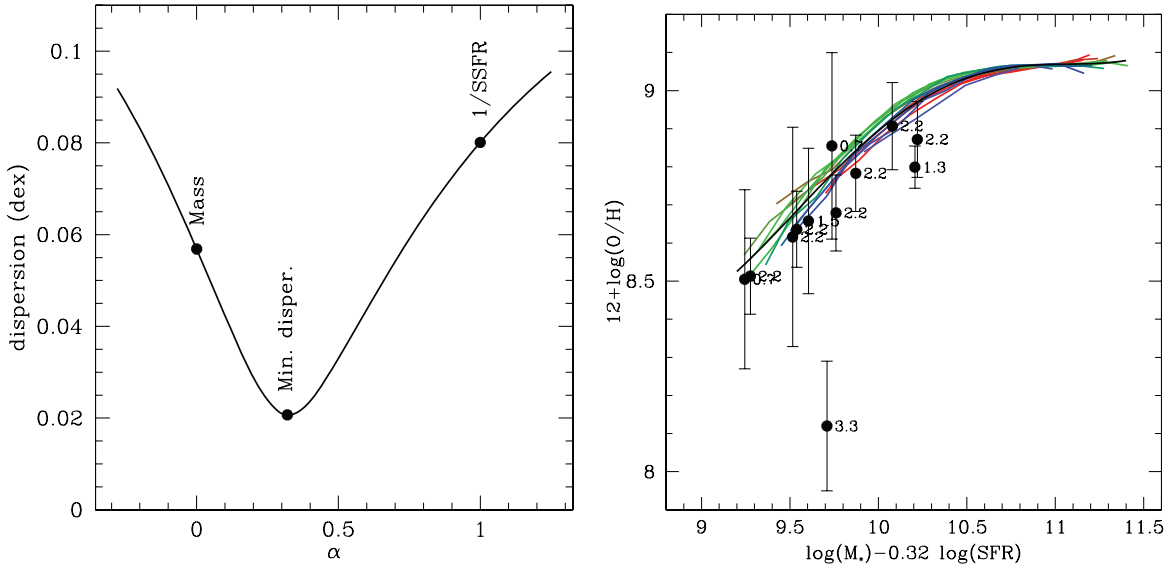

Figure 5. Left-hand panel: residual dispersion of the median values of metallicity of SDSS galaxies as a function of α as defined in equation (3). The values corresponding to the minimum dispersion ($\alpha = 0.32$), to $\alpha = 0$ [$\mu_\alpha = \log(M_\star)$] and to $\alpha = 1$ [$\mu_\alpha = -\log(\mathrm{SSFR})$] are shown. Right-hand panel: metallicity as a function of $\mu_{0.32}$, which minimizes the residual scatter. Coloured lines are local SDSS galaxies, with colours as in the left-hand panel of Fig. 1. The black line shows the polynomial best fit. Black dots are high-redshift galaxies, labelled with redshifts. These galaxies, except those at $z \sim 3.3$, appear to follow the same relation defined by SDSS galaxies.

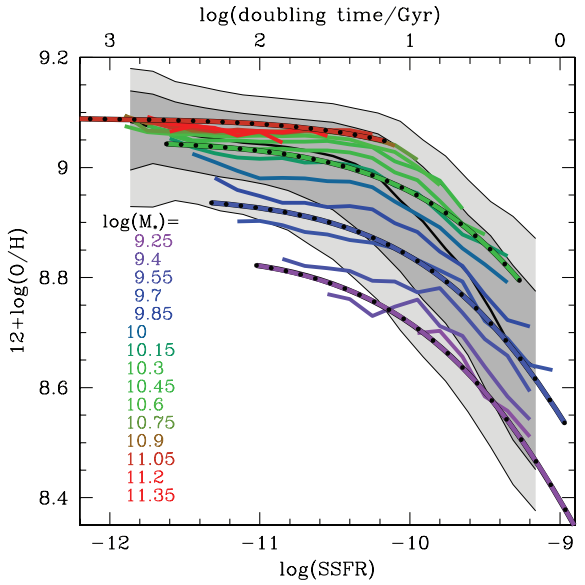

Figure 6. Metallicity of SDSS galaxies as a function of SSFR. The grey-shaded areas contain 64 and 90 per cent of all SDSS galaxies, with the thick central line showing the median relation. The coloured lines show the median metallicities for different values of $M_\star$. The lines with black dots show fits to these metallicity distribution for four values of $\log(M_\star)$, 9.4, 9.7, 10 and 10.9. The model is described in Section 7.1 and includes only dilution for infalling gas and the SK law.

this plot it can be seen that SDSS galaxies of any mass have the same dependence of metallicity on SSFR. A threshold SSFR exists, about $10^{-10}\,\mathrm{yr}^{-1}$ which discriminates the abundance effect of the SFR. Above this limit, metallicity decreases rapidly with SFR in galaxies on any mass. Below this limit, metallicity is constant in massive galaxies [$\log(M_\star) > 10.5$] and slowly decreasing with SFR in less massive galaxies. The interpretation of this behaviour is given in the next section.

The fraction of galaxies above and below this SSFR threshold changes with $M_\star$. Most of the low-mass galaxies, and only a small fraction of high-mass galaxies in our SDSS sample are in the 'high-SSFR' regime, and this is the well-known 'downsizing' effect (Cowie et al. 1996; Gavazzi & Scodeggio 1996). As $M_\star$ and SFR are independent variables of the FMR, downsizing does not shape the relation but defines how it is populated, i.e. how many galaxies of a given $M_\star$ have a certain level of SFR and, as a consequence, metallicity.

7 DISCUSSION

In Section 4 we have shown that in the local universe a tight relation exists between metallicity, stellar mass and SFR, in which metallicity increases with $M_\star$ and decreases with SFR in a systematic way. In Section 5 we have shown that the same relation, without any evolution, holds up to $z = 2.5$, and that the observed evolution of the mass–metallicity relation is simply due to the sampling of different parts of this relation at different redshifts. In Section 6 we have seen that the systematic dependence of metallicity on $M_\star$ and SFR at all redshifts can be expressed in an easy form by introducing the quantity $\mu_{0.32}$, linear combination of $M_\star$ and SFR.

The interpretation of these results must take into account several effects. In principle, metallicity is a simple quantity as it is dominated by three processes: star formation, infall and outflow. If the scaling laws of each of these three processes are known, the dependence of metallicity on SFR and $M_\star$ can be predicted. In practice, these three processes have a very complex dependence of the properties of the galaxies, and can introduce scaling relations in many different ways.

First, it is not known how *outflows* depend on the properties of the galaxies. In many models, star formation produces SNe which inject energy, radiation and momentum into the interstellar medium, with the result of ejecting part of the enriched gas (Veilleux, Cecil & Bland-Hawthorn 2005; Spitoni et al. 2010). A central AGN can also provide feedback (Somerville et al. 2008). The properties of

this galactic winds are debated. Dekel & Woo (2003) reproduced the mass–metallicity relation with a wind related to the energy of SNe, which is proportional to stellar mass. In large galaxies with deep potential wells, such a wind is not effective in producing an outflow (Tremonti et al. 2004). Murray, Quataert & Thompson (2005), Davé, Finlator & Oppenheimer (2007) and Oppenheimer & Davé (2008) discuss a different scheme, the 'momentum-driven wind', in which wind speed increases with galaxy mass while its efficiency decreases.

Secondly, *infalls* are expected to influence metallicity in two ways. On the one hand, infall of metal-poor gas directly reduces the observed metallicity by diluting the metal-rich gas, as discussed, for example, by Finlator & Davé (2008) in the context of their wind scheme. On the other hand, infall is expected to produce star formation activity following the Schmidt–Kennicutt (SK) law, and the metals produced by new stars are expected to increase metallicity. If merging between galaxies, rather than smooth infall from the intergalactic medium, is the main channel to drive gas into galaxies, the fuel of star formation can be significantly enriched, and the dilution effect could be absent.

Thirdly, in some semi-analytical models of galaxy formation (de Rossi, Tissera & Scannapieco 2007; Mouchine et al. 2008) the behaviour of metallicity is dominated by the dependence of *star formation efficiency* of galaxy mass: less massive galaxies are less evolved and therefore show lower metallicities. Some other models (Brooks et al. 2007; Dayal et al. 2009; Salvaterra et al. 2009) put together downsizing and feedback: metallicity is mainly related to different star formation efficiencies in different galaxies, but the efficiency is regulated by SN feedback. Tassis, Kravtsov & Gnedin (2008) not only agree that low star formation efficiency in low-mass galaxies is the main driver of the mass–metallicity relation, but also pointed out that mixing of heavy elements in the outer regions of galaxies could help hiding a significant fraction of metals. Also Köppen et al. (2007) attribute the different abundances to different levels of productions of metals, but their model include systematic variation of IMF, which is proposed to be more top-heavy in galaxies with higher SFRs.

A full exploitation of our results requires a full discussion of these models, that is beyond the scope of this paper and will be subject of a future work. Here we discuss some simple implications of our results on the role and the properties of infalls and outflows. In the next two subsections we will assume two limiting cases for the time-scale of chemical enrichment as compared to the other relevant time-scales.

7.1 The effect of the infall

The dependence of metallicity on SFR can be explained by the dilution effect of the infalling gas. In a very simple model, we assume that galaxies with low SFR have a given gas fraction $f_{\rm g}$. When a certain amount $M_{\rm inf}$ of metal-poor gas is accreted, galaxies start forming stars at a given SFR defined by the SK law on the infalling gas. This is an empirical relation between surface densities of star formation and surface density of gas:

$$\Sigma_{\rm SFR} \sim \Sigma_{\rm gas}^{n}, \tag{6}$$

where n has values around 1.4–1.5 both at low and high redshifts (Kennicutt 1998; Bouché et al. 2007; Kennicutt 2008; Gnedin & Kravtsov 2010; Verley et al. 2010). For SDSS galaxies, the spectroscopic aperture is always the same and the SK law becomes a relation between masses, obtaining

$$\mathrm{SFR} \sim M_{\rm inf}^{n}. \tag{7}$$

In this model, galaxies are observed during the phase when the dilution effect of the infall is predominant over the metallicity enrichment due to new stars, i.e. the observed metallicity $[12 + \log(\mathrm{O/H})]_{\rm obs}$ is related to the initial metallicity $[12 + \log(\mathrm{O/H})]_{\rm in}$ by the ratio of pre-existing and infalling gas:

$$[12 + \log(\mathrm{O/H})]_{\rm obs} = [12 + \log(\mathrm{O/H})]_{\rm in} - \log\left(1 + \frac{M_{\rm inf}}{f_{\rm g}\, M_{\star}}\right). \tag{8}$$

The results of this simple model are presented in Fig. 6. For simplicity, only four values of mass are shown, using the best-fitting values of $f_{\rm g} = 0.3$ per cent and $M_{\rm inf}$ between $10^{5.5}$ and $10^{7.5}\mathrm{M}_{\odot}$. This range of values of $M_{\rm inf}$ is the same for all masses and is determined by the range of observed SSFR. For each mass, the metallicity level at low SSFR, $[12 + \log(\mathrm{O/H})]_{\rm in}$, is a free parameter, whose value is possibly determined by other effects, such as outflow. Our very simple model is capable of reproducing all the main properties of the FMR: metallicity reduces with increasing SFR, a threshold of SSFR exists, larger metallicity effects are produced in smaller galaxies, both above and below the threshold, and the slope of the relation at high SSFR is exactly as observed.

For this scenario to work, the time-scales of chemical enrichment must be longer than the dynamical scales of the galaxies, over which the SFR is expected to evolve. In other words, galaxies on the FMR are in a *transient phase*: after an infall, galaxies first evolve towards higher SFR and lower metallicities. Later, while gas is converted into stars and new metals are produced, either galaxies drop out of the sample because they have faint Hα, or evolve towards higher values of $\mu_{0.32}$ and higher metallicities along the FMR. A detail modelling of this evolution and a comparison of the different time-scales involved is needed to test if this is a viable explanation.

In this scenario, the dependence of metallicity on SFR is due to infall and dominates at high redshifts, where galaxies with massive infalls and large SFRs are found. In contrast, in the local universe such galaxies are rare, most of the galaxies have low level of accretion, and abundances are dominated by the dependence on mass, possibly due to outflow.

7.2 Properties of outflows

In many local galaxies, time-scales of chemical enrichment can be shorter than the other relevant time-scales (e.g. Silk 1993), and galaxies can be in a *quasi-steady-state situation*, in which gas infall, star formation and metal ejection occur simultaneously (Bouche et al. 2009). This is the opposite situation of what is discussed in the previous section.

Assuming this quasi-steady-state situation, in which infall and SFR are slowly evolving with respect to the time-scale of chemical enrichment, our results can be used to derive information on the mechanisms of infall and outflow. Fig. 6 implies that a process exists that depends only on SSFR which is effective in reducing metallicity from a level that depends on mass. In a steady-state situation, infall cannot be the only dominant effect. The exponent n of the SK relation is larger than 1, and this means that the efficiency of star formation increases with gas density, i.e. more active galaxies should also be more efficient in converting metal-poor gas into stars. As a consequence, the SK law alone, applied to the infalling gas, would predict the opposite to what is actually observed, i.e. metallicities increasing with SFR at constant mass. Some other effect must be present.

One obvious candidate is the presence of outflows, as usually observed in starburst galaxies and discussed by many authors. As discussed above, there are several possible types of galactic winds, which follow different scaling relations with mass and SFR. When the dilution by the infalling gas $M_{\rm inf}$ is considered together with enrichment due to the SFR, we can reproduce the dependence of metallicity on $\mu_{0.32}$ by introducing an outflow proportional to $\mathrm{SFR}^s\ M_\star^{-m}$, with s and m free parameters. In this case, at the first order we obtain

$$12 + \log(\mathrm{O/H}) \sim \log\left(\frac{\mathrm{SFR}}{M_{\rm inf}\,\mathrm{SFR}^s\,M_\star^{-m}}\right) \quad (9)$$

and, using the SK law

$$12 + \log(\mathrm{O/H}) \sim m\log(M_\star) + \left(1 - \frac{1}{n} - s\right)\log(\mathrm{SFR}), \quad (10)$$

where $n = 1.5$ is the index of the SK law. This is the functional form of μ_α, and comparing this equation with the best-fitting value of $\alpha = 0.32$ we obtain $m = 1$ and $s = 0.65$. In other words, in a steady-state situation the outflow must be inversely proportional to mass and must increase with $\mathrm{SFR}^{0.65}$.

We note that, using an index n of the SK relation of 1.5, the best-fitting value of $\alpha = 0.32$ corresponds almost exactly to $1-1/n = 0.33$. Using this, the simplest way to combine the relevant physical parameters to produce $\mu_{0.32}$ is

$$\log\left(\frac{M_{\rm inf}\,M_\star}{\mathrm{SFR}}\right) \sim \log(M_\star) - (1 - 1/n)\log(\mathrm{SFR}) \sim \mu_{0.32}. \quad (11)$$

In this form, metallicity increases with $M_\star$, an effect easily attributable either to downsizing or to outflow. In contrast, the dependence of metallicity on $M_{\rm inf}/\mathrm{SFR}$ is not obvious and requires complete modelling.

7.3 Merging and smooth accretion

The small scatter of SDSS galaxies around the FMR derived in Section 4 can be used to constrain the characteristics of gas accretion. For this infall/outflow scenario to work and produce a very small scatter around the FMR, two conditions are simultaneously required: (1) star formation is always associated to the same level of metallicity dilution due to infall of metal-poor gas and (2) there is a relation between the amount of infalling and outflowing gas and the level of star formation. These conditions for the existence of the FMR fits into the smooth accretion models proposed by several groups (Bournaud & Elmegreen 2009; Dekel et al. 2009), where continuous infall of pristine gas is the main driver of the growth of galaxies. In this case, metal-poor gas is continuously accreted by galaxies and converted in stars, and a long-lasting equilibrium between gas accretion, star formation and metal ejection is expected to be established.

In contrast, larger scatters around the FMR are expected in case of merging, for two reasons. First, in interacting systems, a part of the gas producing the starburst could be metal-poor material due to interaction-induced infall (Rupke et al. 2008; Rupke, Kewley & Barnes 2010), but a part of it is expected to be a metal-rich material already present inside the interacting galaxies. In this case the initial dilution is not present, and higher metallicities are expected. This is true, in particular, for the smaller member of a merger between galaxies with very different masses. The secondary, smaller mass galaxy is expected to show higher metallicity because its star formation activity is expected to be fuelled by gas coming from the other, larger, more metal-rich galaxy. This is exactly what is observed by Michel-Dansac et al. (2008): higher metallicities, above the mass–metallicity relation, are present in the secondary member of minor mergers. Secondly, the level of SFR is related to the properties of the merging galaxies, and is expected to vary significantly during the different stages of the interactions. As a consequence, a large range on SFR is expected for a given level of metallicity during the merging history of the systems. Both effects are expected to produce larger spreads in merging galaxies, and this is what is actually observed (Kewley, Geller & Barton 2006; Michel-Dansac et al. 2008; Rupke et al. 2008; Peeples et al. 2009). As discussed in Section 4, the presence of interacting galaxies in the SDSS could be at the origin of the extended wing in the distribution of difference with the FMR, and this point will be investigated in a future paper.

The situation at intermediate redshift, up to $z = 2.5$, is less clear. Galaxies show larger dispersion in metallicity, but this can be explained by larger uncertainties in the measured values of metallicity, mass and SFR. With the present data sample it is not possible therefore to study whether smooth accretion is dominant up to $z = 2.5$ as in the local universe, or if merging has a larger impact on dispersion. Nevertheless, the absence of any evolution of the FMR up to these redshift supports a single physical process of accretion in all these galaxies. At even higher redshift, $z \sim 3.3$, when galaxies show large scatter *and* different average metallicities, it is likely that new physical effects become important.

The uncertainties on SFR can be a critical point. Under this respect, the *Herschel* satellite is expected to improve significantly the accuracy of the estimate of total SFRs in a short time. With its contribution it will be possible to reduce the scatter, especially at high redshifts, study the presence of an intrinsic dispersion of properties among the galaxies and obtain a much better characterization of the FMR relation at high redshifts.

7.4 Origin of the evolution at $z > 2.5$

The interplay between gas accretion, star formation and gas outflow seems to be the same at any redshift up to $z = 2.5$, as all these galaxies follow the same FMR. What is important in this context is the ratio between the different rates and the various time-scale involved: gas infall, dynamical times, star formation, stellar evolution, SN explosion, chemical mixing and outflow. Apparently the relative importance of these processes does not evolve up to $z = 2.5$. It is possible that at higher redshifts this constant balance does not apply any more and lower metallicities are observed while galaxies evolve towards the FMR. This could be related to an increasing importance of merging as a way to drive cold gas into the galaxies, at least in the most luminous objects that are preferentially selected as Lymn-break galaxies (LBG). This point can be addressed by studying the morphology and the mass–SFR relation in these objects.

It should be noted that the metallicity of galaxies at $z = 3.3$ can also be reproduced by the same model in Section 7.1, in which the infall dilution is dominant. Local galaxies are reproduced by $M_{\rm inf}$ of the order of 10^6–$10^7\,\mathrm{M}_\odot$, while gas masses of the order of 10^9–$10^{10}\,\mathrm{M}_\odot$ are needed for galaxies at $z = 3.3$. This is in very good agreement with what was obtained by Mannucci et al. (2009) and Cresci (2010). Also, galaxies at these high redshifts could be preferentially detected during the first stages of the starburst, when the dilution effect is maximum. This is possible if the starburst has a peak on short time-scales, shorter than the time-scales of metal production and chemical mixing, and declines afterwards. Galaxies could also become more dust rich during the later phases of the starburst, and drop out from the UV-selected samples.

8 CONCLUSIONS

We have studied the dependence of gas-phase metallicity $12 + \log(\mathrm{O/H})$ on stellar mass $M_\star$ and SFR on a few samples of galaxies from $z = 0$ to 3.3. In the local universe, we find that metallicity is tightly related to both $M_\star$ and SFR (Fig. 1), and this defines the FMR (Fig. 2). The residual metallicity dispersion of local SDSS galaxies around this FMR is about 0.05 dex (Fig. 3), i.e. about 12 per cent. The well-known mass–metallicity relation, together with the luminosity–metallicity and velocity–metallicity relations, is one particular projection of this relation into one plane, and neglecting the dependence of metallicity on SFR results in doubling the observed dispersion.

When high-redshift galaxies are compared to the FMR defined locally, we find no evolution up to $z = 2.5$, i.e. high-redshift galaxies follow the same FMR defined by SDSS galaxies even if they have higher SFRs (Fig. 4). This means that the same physical processes are in place in the local universe and at high redshifts. The observed evolution of the mass–metallicity relation is due to the increase of the average SFR with redshift, which results in sampling different parts of the same FMR at different redshifts.

At even higher redshift, $z \sim 3.3$, evolution of $\sim$0.6 dex with respect to the FMR is found, although several observational effects and selection biases may affect the size of this evolution. This is an indication that different mechanisms start to dominate.

Even if the nature of the FMR is three dimensional in $M_\star$, SFR and $12 + \log(\mathrm{O/H})$, metallicity is found to be tightly correlated with $\mu_{0.32} = \log(M_\star) - 0.32 \log(\mathrm{SFR})$. Galaxies at any redshifts up to $z = 2.5$ follow the same $\mu_{0.32}$–metallicity relation and have the same range of values of $\mu_{0.32}$ (Fig. 5).

Metallicity in galaxies of any mass is found to have the same dependence of SSFR, with galaxies above the threshold of $\mathrm{SSFR} = 10^{-10}\,\mathrm{yr}^{-1}$ showing a rapidly decreasing metallicities with increasing SSFR (Fig. 6).

The interpretation of the existence of the FMR, its dependence of SSFR, and the role of $\mu_{0.32}$ depend on the relevant time-scales. If dynamical times are shorter than time-scales for chemical enrichment, the dependence of metallicity on SFR can be easily explained by dilution by infall. In this case this effect dominates the metallicity evolution of galaxies at high redshift, when galaxies grow because of massive accretions of metal-poor gas and produce large SFR. Also galaxies at $z = 3.3$ can fit into this scheme, with large masses of infalling gas. This is in agreement with other recent independent results (Mannucci et al. 2009; Cresci 2010). In the local universe, galaxies with large SFR are rare and often associated to merging events, and other effects become dominant which relate metallicity mainly to $M_\star$. Outflow is a possibility, although downsizing could also work. If, in contrast, infall and SFR evolve on time-scales much longer than the chemical enrichment time-scale, a sort of steady-state situation is created: continuous infall of metal-poor gas, which both sustains SFR and dilutes metallicity, and outflow of metal-rich gas in galactic winds. In this case the outflows must depend on both mass and SFR.

The small residual scatter around the FMR in the local universe supports the smooth accretion scenario, where galaxy growth is dominated by continuous accretion of cold gas. Interacting and merging galaxies are expected to show larger spread around the FMR, in agreement to what is actually observed. Galaxies at intermediate and high redshifts show larger metallicity dispersions, which could be due either to uncertainties in the measurements, or to intrinsic dispersion, or both. This effect prevents us to study the evolution of residual scatter with redshift. Nevertheless, the absence of significant biases in metallicity or in SFR up to $z = 2.5$ points towards the existence of the same physical effects and the dominance of smooth accretion even at intermediate redshift.

ACKNOWLEDGMENTS

We are grateful to the MPA/JHU teams which made their measured quantities on SDSS galaxies publicly available, and to the members of the Italian Virtual Observatory for support on data visualization. We also acknowledge stimulating discussions with T. Nagao, R. Davé, S. Ellison and the Arcetri MEGA group.

REFERENCES

Abazajian K. N. et al., 2009, ApJS, 182, 543
Agertz O., Teyssier R., Moore B., 2009, MNRAS, 397, L64
Bouché N. et al., 2007, ApJ, 671, 303
Bouche N. et al., 2009 (arXiv e-prints)
Bournaud F., Elmegreen B. G., 2009, ApJ, 694, L158
Brinchmann J., Charlot S., White S. D. M., Tremonti C., Kauffmann G., Heckman T., 2004, MNRAS, 351, 1151
Brinchmann J., Pettini M., Charlot S., 2008, MNRAS, 385, 769
Brooks A. M., Governato F., Booth C. M., Willman B., Gardner J., Wadsley J., Stinson G., Quinn T., 2007, ApJ, 655, L17
Brooks A. M., Governato F., Quinn T., Brook C. B., Wadsley J., 2009, ApJ, 694, 396
Calura F., Pipino A., Chiappini C., Matteucci F., Maiolino R., 2009, A&A, 504, 373
Calzetti D., Armus L., Bohlin R. C., Kinney A. L., Koornneef J., Storchi-Bergmann T., 2000, ApJ, 533, 682
Chabrier G., 2003, PASP, 115, 763
Charlot S., Longhetti M., 2001, MNRAS, 323, 887
Cowie L. L., Barger A. J., 2008, ApJ, 686, 72
Cowie L. L., Songaila A., Hu E. M., Cohen J. G., 1996, AJ, 112, 839
Cresci G. et al., 2010, Nat, submitted
Daddi E. et al., 2007, ApJ, 670, 156
Davé R., Finlator K., Oppenheimer B. D., 2007, in Emsellem E., Wozniak H., Massacrier G., Gonzalez J.-F., Devriendt J., Champavert N., eds, EAS Publ. Ser. Vol. 24, CRAL-2006, Chemodynamics: From First Stars to Local Galaxies. EDP Sciences, Paris, p. 183
Davé R., Finlator K., Oppenheimer B. D., Fardal M., Katz N., Keres D., Weinberg D. H., 2010, MNRAS, 404, 1355
Dayal P., Ferrara A., Saro A., Salvaterra R., Borgani S., Tornatore L., 2009, MNRAS, 400, 2000
de Rossi M. E., Tissera P. B., Scannapieco C., 2007, MNRAS, 374, 323
Dekel A., Woo J., 2003, MNRAS, 344, 1131
Dekel A., Sari R., Ceverino D., 2009, ApJ, 703, 785
Edmunds M. G., 1990, MNRAS, 246, 678
Ellison S. L., Patton D. R., Simard L., McConnachie A. W., 2008, ApJ, 672, L107
Epinat B. et al., 2009, A&A, 504, 789
Erb D. K., 2008, ApJ, 674, 151
Erb D. K., Shapley A. E., Pettini M., Steidel C. C., Reddy N. A., Adelberger K. L., 2006, ApJ, 644, 813
Finlator K., Davé R., 2008, MNRAS, 385, 2181
Förster Schreiber N. M. et al., 2009, ApJ, 706, 1364
Garnett D. R., 2002, ApJ, 581, 1019
Gavazzi G., Scodeggio M., 1996, A&A, 312, L29
Gnedin N. Y., Kravtsov A. V., 2010, ApJ, 714, 287
Hainline K. N., Shapley A. E., Kornei K. A., Pettini M., Buckley-Geer E., Allam S. S., Tucker D. L., 2009, ApJ, 701, 52
Hayashi M. et al., 2009, ApJ, 691, 140
Kauffmann G. et al., 2003a, MNRAS, 341, 33
Kauffmann G. et al., 2003b, MNRAS, 346, 1055
Kennicutt R. C., Jr, 1998, ARA&A, 36, 189

Kennicutt R. C., Jr, 2008, in Knapen J. H., Mahoney T. J., Vazdekis A., eds, ASP Conf. Ser. Vol. 390, Pathways Through an Eclectic Universe. Astron. Soc. Pac., San Francisco, p. 149
Kewley L. J., Ellison S. L., 2008, ApJ, 681, 1183
Kewley L. J., Geller M. J., Barton E. J., 2006, AJ, 131, 2004
Kobayashi C., Springel V., White S. D. M., 2007, MNRAS, 376, 1465
Köppen J., Weidner C., Kroupa P., 2007, MNRAS, 375, 673
Kroupa P., 2001, MNRAS, 322, 231
Law D. R., Wright S. A., Ellis R. S., Erb D. K., Nesvadba N., Steidel C. C., Swinbank M., 2009, preprint
Lee H., Skillman E. D., Cannon J. M., Jackson D. C., Gehrz R. D., Polomski E. F., Woodward C. E., 2006, ApJ, 647, 970
Lehnert M. D., Heckman T. M., 1996, ApJ, 462, 651
Lehnert M. D., Nesvadba N. P. H., Tiran L. L., Matteo P. D., van Driel W., Douglas L. S., Chemin L., Bournaud F., 2009, ApJ, 699, 1660
Lequeux J., Peimbert M., Rayo J. F., Serrano A., Torres-Peimbert S., 1979, A&A, 80, 155
Liu X., Shapley A. E., Coil A. L., Brinchmann J., Ma C.-P., 2008, ApJ, 678, 758
Lopez-Sanchez A. R., 2010, preprint
Magrini L., Sestito P., Randich S., Galli D., 2009, A&A, 494, 95
Maiolino R. et al., 2008, A&A, 488, 463
Mannucci F. et al., 2009, MNRAS, 398, 1915
McClure R. D., van den Bergh S., 1968, AJ, 73, 1008
Michel-Dansac L., Lambas D. G., Alonso M. S., Tissera P., 2008, MNRAS, 386, L82
Mouchine M., Gibson B. K., Renda A., Kawata D., 2008, preprint
Moustakas J., Kennicutt R. C., Jr, Tremonti C. A., 2006, ApJ, 642, 775
Murray N., Quataert E., Thompson T. A., 2005, ApJ, 618, 569
Nagao T., Maiolino R., Marconi A., 2006, A&A, 459, 85
Oppenheimer B. D., Davé R., 2008, MNRAS, 387, 577
Panter B., Jimenez R., Heavens A. F., Charlot S., 2008, MNRAS, 391, 1117
Peeples M. S., Pogge R. W., Stanek K. Z., 2009, ApJ, 695, 259
Pérez-González P. G., Gil de Paz A., Zamorano J., Gallego J., Alonso-Herrero A., Aragón-Salamanca A., 2003, MNRAS, 338, 525
Pérez-Montero E. et al., 2009, A&A, 495, 73
Pilyugin L. S., Vílchez J. M., Contini T., 2004, A&A, 425, 849
Rodrigues M. et al., 2008, A&A, 492, 371
Rupke D. S. N., Veilleux S., Baker A. J., 2008, ApJ, 674, 172
Rupke D. S. N., Kewley L. J., Barnes J. E., 2010, ApJ, 710, L156
Salim S. et al., 2007, ApJS, 173, 267
Salvaterra R., Ferrara A., Dayal P., 2009, Nat, 461, 1258
Savaglio S. et al., 2005, ApJ, 635, 260
Scannapieco C., Tissera P. B., White S. D. M., Springel V., 2008, MNRAS, 389, 1137
Schiminovich D. et al., 2007, ApJS, 173, 315
Shapley A. E., Coil A. L., Ma C.-P., Bundy K., 2005, ApJ, 635, 1006
Silk J., 1993, Proc. Natl. Acad. Sci., 90, 4835
Somerville R. S., Hopkins P. F., Cox T. J., Robertson B. E., Hernquist L., 2008, MNRAS, 391, 481
Spitoni E., Calura F., Matteucci F., Recchi S., 2010, A&A, 514, A73
Tassis K., Kravtsov A. V., Gnedin N. Y., 2008, ApJ, 672, 888
Tremonti C. A. et al., 2004, ApJ, 613, 898
Veilleux S., Cecil G., Bland-Hawthorn J., 2005, ARA&A, 43, 769
Verley S., Corbelli E., Giovanardi C., Hunt L. K., 2010, A&A, 510, A64
Wright S. A., Larkin J. E., Law D. R., Steidel C. C., Shapley A. E., Erb D. K., 2009, ApJ, 699, 421
Wright S. A., Larkin J. E., Graham J. R., Ma C., 2010, ApJ, 711, 1291

This paper has been typeset from a TEX/LATEX file prepared by the author.